THE ASTROPHYSICAL JOURNAL, 565:1017–1021, 2002 February 1
© 2002. The American Astronomical Society. All rights reserved. Printed in U.S.A.

UNUSUAL DIFFUSE X-RAY SOURCE IN THE GALACTIC CENTER REGION

ATSUSHI SENDA, HIROSHI MURAKAMI, AND KATSUJI KOYAMA
Department of Physics, Graduate School of Science, Kyoto University, Sakyo-ku, Kyoto 606-8502, Japan;
senda@cr.scphys.kyoto-u.ac.jp, hiro@cr.scphys.kyoto-u.ac.jp, koyama@cr.scphys.kyoto-u.ac.jp
Received 2001 June 9; accepted 2001 September 28

ABSTRACT

We report the *ASCA* and *Chandra* discovery of a diffuse X-ray source in the Galactic center region. The X-ray spectrum is fitted with a nonequilibrium ionization (NEI) plasma model with a temperature of about 6 keV. The model requires higher than solar metal abundances, a young plasma age of $\simeq 100$ yr, and a large $N_{\rm H}$ value of about 10^{23} cm^{-2}. The $N_{\rm H}$ value constrains the source position to be in the Galactic center region at a distance of about 8.5 kpc. The high resolution X-ray image with the *Chandra* ACIS shows a ring of 10″ radius, which corresponds to 0.4 pc at the Galactic center, and a tail-like structure. Although the morphology is peculiar, the other X-ray features are likely to be a very young supernova remnant, possibly in a free expansion phase.

Subject headings: Galaxy: center — ISM: individual (G0.570−0.018, CXO J 174702.6−282733) — supernova remnants — X-rays: ISM

1. INTRODUCTION

The Galactic center (GC) region within $\simeq 100$ pc is very rich in various X-ray sources such as X-ray binaries, young stellar clusters, and supernova remnants (SNRs). A big mystery is a diffuse hot ($\simeq 10$ keV) plasma of $1^\circ \times 2^\circ$ elliptical shape with a total energy of about 10^{54} ergs (Koyama et al. 1989, 1996; Yamauchi et al. 1990). The dynamical age of the hot plasma is estimated to be about 10^5 yr. One possible origin of the diffuse plasma is multiple supernova explosions (10^3 supernovae) in the past 10^5 yr (Yamauchi et al. 1990), which predicts that many young SNRs should be discovered with a deep exposure above the 2 keV X-ray band. With the *ASCA* Galactic center survey project, we found an extended X-ray source on the Galactic plane near the giant molecular cloud Sgr B2, which exhibits unusually strong iron lines (Sakano et al. 1999). The *Chandra* Cycle 1 observation confirmed the *ASCA* results and revealed a ring and tail structure in the iron Kα line band, which we named G0.570−0.018/CXO J174702.6−282733 (hereafter, G0.570−0.018). This paper reports the *ASCA* and *Chandra* results of G0.570−0.018 and discusses the nature of this peculiar source.

2. OBSERVATIONS AND DATA REDUCTIONS

ASCA (Tanaka et al. 1994) observed the Sgr B2 region near the Galactic center on 1993 October 1 (PV phase) and 1994 September 22–24 (AO2). *ASCA* was equipped with two Gas Imaging Spectrometers (GIS2 and GIS3) and two Solid-State Imaging Spectrometers (SIS0 and SIS1) on the focal planes of four X-ray telescopes (XRTs) (Selemitsos et al. 1995; Ohashi et al. 1996; Burke et al. 1991). In both observations, G0.570−0.018 was placed on the center of the SIS field and, hence, was intercepted by the center gap of each CCD chip. We therefore used the GIS (GIS2 and GIS3) data only. For GISs, nominal bit assignment of PH mode was used in high and medium bit rate. After the standard data screening, we obtained the effective exposure time of PV and AO2 of 17.5 and 80.0 ks, respectively.

G0.570−0.018 was in the ACIS-I field of view when *Chandra* observed the Sgr B2 region on 2000 March 29–30. The satellite and instruments are described by Weisskopf et al. (1996) and G. P. Garmire et al. (2001, in preparation), respectively. Data reduction is made with the same method of the Sgr B2 analysis (Murakami, Koyama, & Maeda 2001). G0.570−0.018 is located at the top of chip I3 and thus is heavily affected by the charge transfer inefficiency (CTI). To minimize the effect of the CTI degradation, we use the software developed by Townsley et al. (2000). We correct the energy gain using the instrumental emission line from Ni (Kα = 7.5 keV) and Au atoms (Lα = 9.7 keV) with an accuracy of less than 0.5% (90% confidence). The response matrix is made using the nearly contemporaneous observation of reference lines from an onboard calibration source (OBSID = 62097), which are analyzed with the same CTI correction. The effective area of the telescope mirrors and the detection efficiency of ACIS are calculated with the *mkarf* program in the Chandra Interactive Analysis of Observations Software (CIAO, Version 2.1). After screening the data, we obtain the effective exposure time of 100 ks.

3. RESULTS AND ANALYSIS

3.1. *X-Ray Morphology*

In the *ASCA* GIS image pointed at the Sgr B2 cloud, we find a local excess in the west of Sgr B2. This excess is clearly seen if we limit the X-ray energy band of 6.0–7.0 keV, which includes the iron K-shell transition line. Figure 1 shows the 6.0–7.0 keV band image. The brightest source located at the northeast is the giant molecular cloud Sgr B2 (Murakami et al. 2000). The other excess at the center of the image is a newly discovered X-ray source. Because of the limited statistics and spatial resolution, error of the peak position of the diffuse structure is rather large, in the range of $0^\circ.55 \lesssim l \lesssim 0^\circ.57$, $-0^\circ.02 \lesssim b \lesssim 0^\circ.00$.

In order to investigate the accurate position and fine spatial structure of this diffuse source, we inspect the *Chandra* image in the 4.0–7.0 keV band. As is shown in Figure 2, we see a complex X-ray structure with a ring of about 10″ radius and an east-to-west tail from the ring. The center coordinate of the ring structure is R.A. = $17^{\rm h}47^{\rm m}02^{\rm s}.6$, decl. = $-28^\circ 27' 33''$ (epoch 2000.0), which corresponds to $(l, b) = (0^\circ.570, -0^\circ.018)$, the same position of the *ASCA* diffuse source within the error. We hence designate this source as G0.570−0.018/CXO J174702.6−282733 (G0.570−0.018). To investigate the statistical significance of

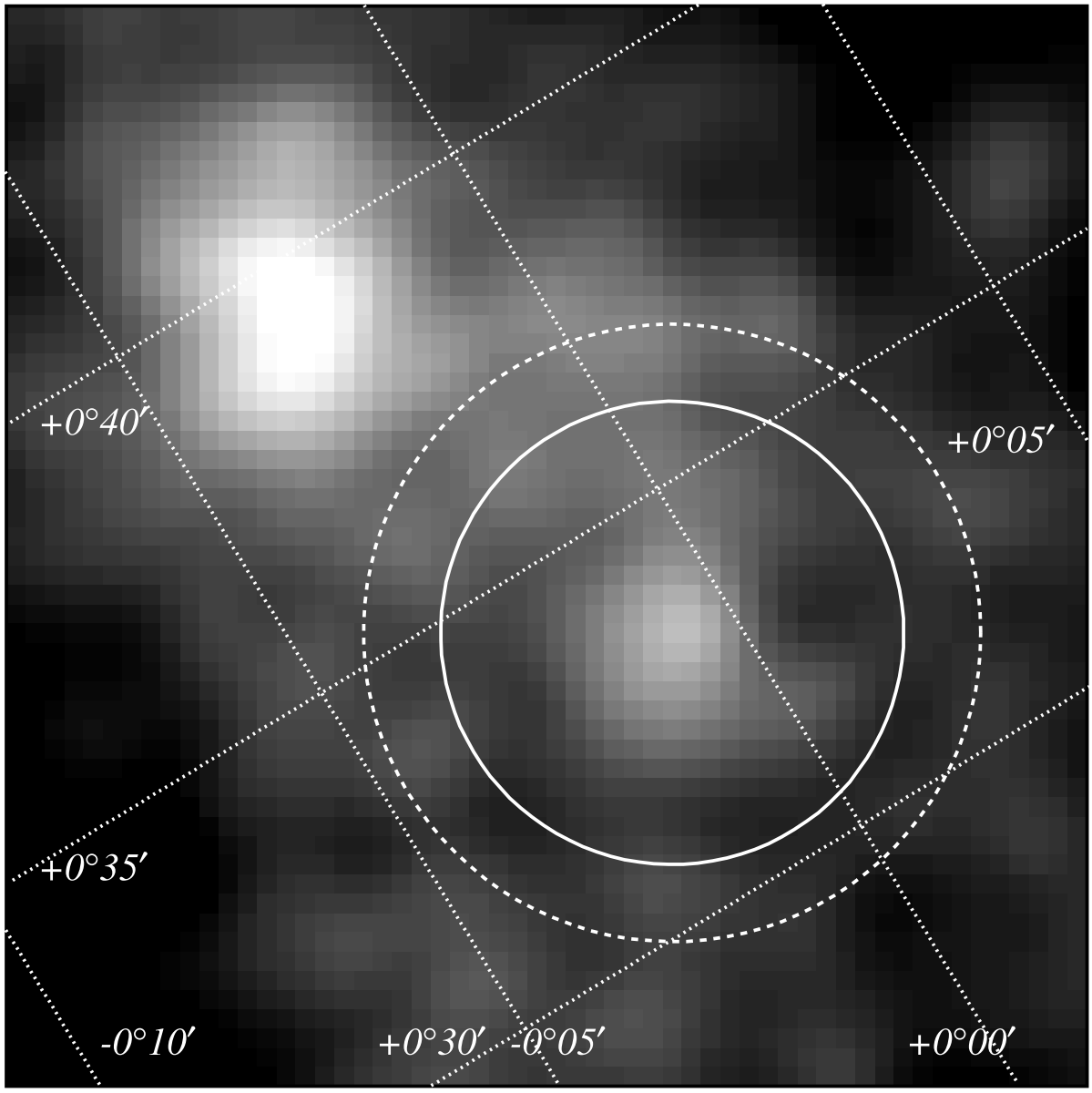


FIG. 1.—*ASCA* GIS image in the 6.0–7.0 keV (iron line) band. The dotted lines are the Galactic coordinates with grid spacing of 5′. The source at the lower right is G0.570−0.018, and the spectrum is taken from the solid circle of a 3′ radius. The background spectrum is taken from the annulus defined by the solid and dashed (radius = 4′) circles. The brightest source in the upper left is the Sgr B2 cloud.

the shell-like structure, we make a radial profile with the center at ($17^h47^m02^s.6$, $-28°27'33''$; J2000.0). Figure 3 shows the radial profile in the 4.0–7.0 keV band. The excess around 10″ is statistically significant, hence the ring structure is real. On the other hand, a faint pointlike structure at the shell center seen in Figure 2 is not significant because it contains only 3 photons. Unlike Sgr B2, neither radio nor any other wave band counterpart is found for G0.570−0.018 (see Oka et al. 1998a, 1998b; Tsuboi, Handa, & Ukita 1999; Lis & Carlstrom 1994; Mehlinger et al. 1992, 1993; Seiradakis et al. 1989).

3.2. *X-Ray Spectra*

The *ASCA* X-ray spectrum is made using the data in a circle of 3′ radius and subtracting the background data in a $3' < r < 4'$ ring, as is shown in Figure 1. The spectrum exhibits a prominent line at 6.0–7.0 keV and large absorption at the low-energy band. We then fit it with a phenomenological model of a thermal bremsstrahlung plus a Gaussian line. The line energy is determined to be $6.60^{+0.12}_{-0.09}$ keV with the equivalent width of $3.7^{+3.0}_{-1.2}$ keV (hereafter, errors are at the 90% confidence level unless otherwise noted), indicating a Kα line from iron atoms with lower ionization states than helium-like (6.7 keV). The temperature is constrained to be higher than 2 keV. Therefore, the equilibrium ionization state of iron should be helium- or hydrogen-like with the line energy of 6.7–6.9 keV. We thus conclude that the plasma is still in an ionizing phase or in a nonequilibrium ionization (NEI).

The *Chandra* X-ray spectrum is made from the same area as with *ASCA*, while the background spectrum is taken from a source-free region with the same CTI effect as the source region. The background-subtracted flux is 20,400 counts, and the spectrum shows a clear iron line as is

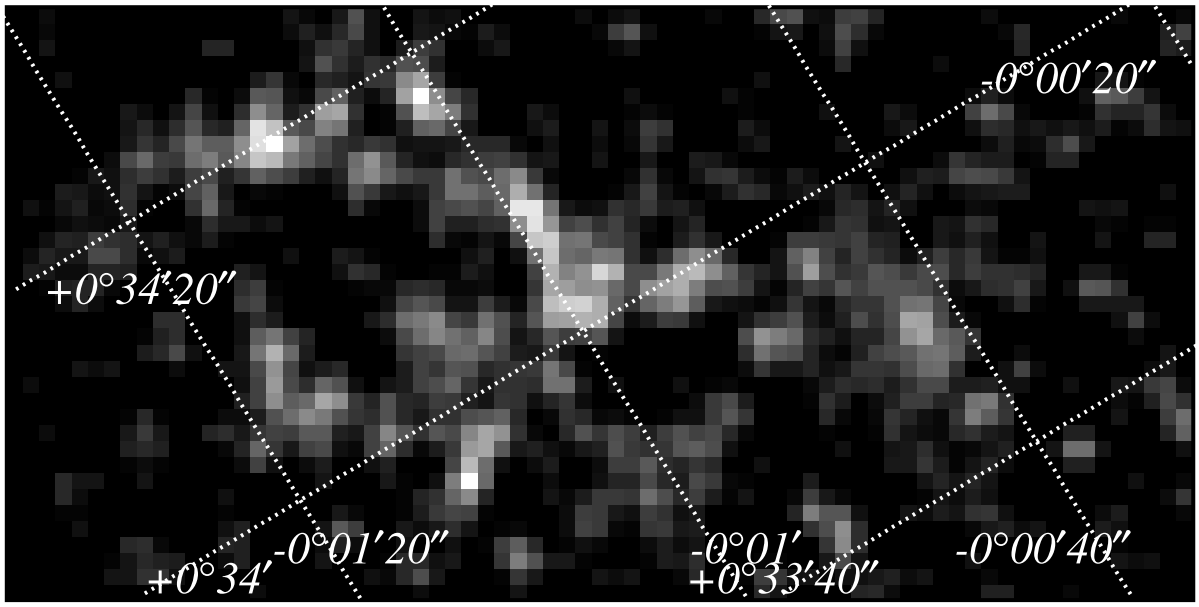


FIG. 2.—*Chandra* ACIS-I image of G0.570−0.018 in the 4.0–7.0 keV band. The dotted lines are the Galactic coordinates with grid spacing of 20″. G0.570−0.018 is seen to be a 10″ radius ring with an east-west tail. This image is smoothed with a Gaussian of $\sigma = 2$ pixels. Before the smoothing, the brightest pixel has 3 photons. The brightness increases with a linear scale from 0.1 (*black pixels*) to 1.3 photons (*white pixels*).

already found with *ASCA*. In the diffuse source region, we also find many faint pointlike sources. We hence execute the CIAO *wavdetect* software of a wavelet method (Freeman et al. 2000) and resolve 18 point sources. The integrated flux (2.0–10.0 keV) of all the point sources is 410 counts, which is only $\simeq 2\%$ of the diffuse X-rays. Therefore, a contamination of the point sources can be ignored in practice. The *Chandra* spectrum is well fitted with the same phenomenological model as used for the *ASCA* spectrum: a bremsstrahlung plus a Gaussian line. The plasma temperature is constrained to be greater than 3.4 keV, while the line energy is 6.50 ± 0.03 keV with an equivalent width of $4.1^{+1.4}_{-1.0}$ keV. Thus, the best-fit parameters are consistent with, and are more accurate than, the *ASCA* results.

Since both the *ASCA* and *Chandra* spectra are fitted with the same model, and the line center energy is consistent with an NEI plasma, we simultaneously fitted the two spectra with a more realistic NEI plasma model (Borkowski et al. 2001). In addition to a conventional thin thermal plasma model, an NEI model includes another parameter, which is called the ionization parameter $\tau = nt$, where n and t are plasma density and elapsed time after the plasma is heated up. As the parameter τ becomes larger than 10^{12}–10^{13} cm^{-3} s, an NEI plasma becomes a collisional ionization equilibrium (CIE) plasma. In addition to the strong iron line, the *Chandra* spectrum includes emission lines at the energies of K-shell transition of argon and calcium atoms. We therefore vary the abundances of all the elements

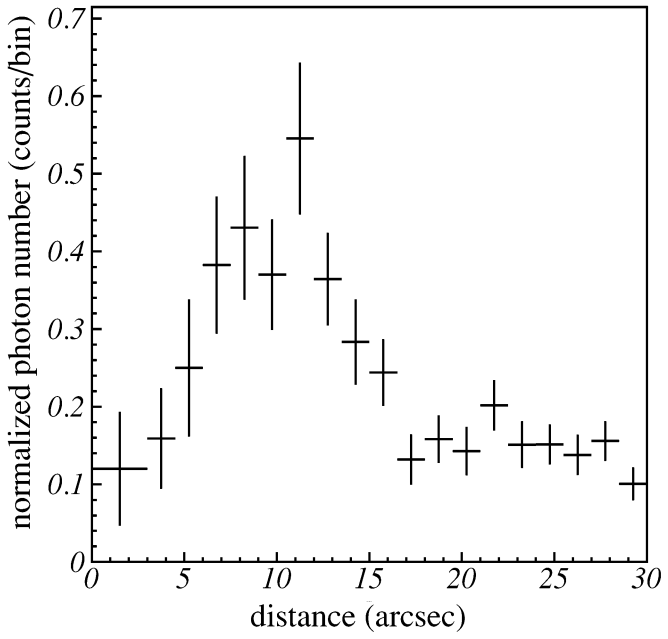


FIG. 3.—Radial profile of the ring structure of G0.570−0.018. The ring center is ($17^h47^m02^s.6$, $-28°27'33''$; J2000.0).

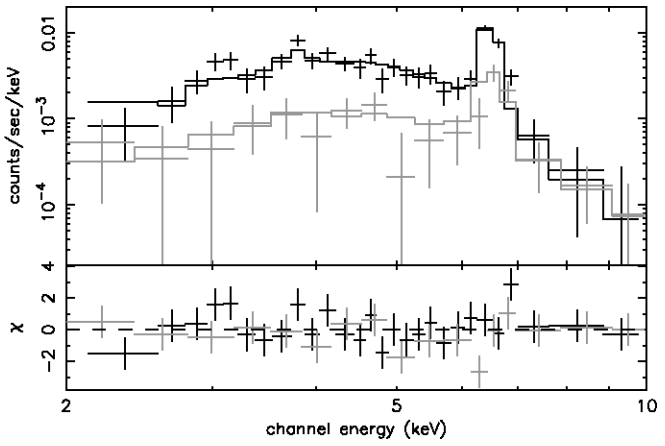


FIG. 4.—X-ray spectra of G0.570−0.018 obtained from *ASCA* (*gray*) and *Chandra* (*black*). The data points are shown by crosses, while the solid lines show the best-fit NEI plasma model. The data residuals are shown in the lower panel.

TABLE 1

BEST-FIT PARAMETERS OF NEI MODEL OBTAINED FROM THE COMBINED FIT OF THE *ASCA* AND *Chandra* SPECTRA

Parameter	Value
N_H[a]	13.9 (10.7–17.2) $\times 10^{22}$ H cm^{-2}
kT[b]	6.1 (3.1–25.8) keV
nt[c]	1.7 (1.3–2.7) $\times 10^{10}$ s cm^{-3}
Metal abundances[d]	4.5 (1.6–9.9) solar
Flux[e]	8.2 $\times 10^{-13}$ergs cm^{-2} s^{-1}
L_X[f]	1.3 $\times 10^{34}$ ergs s^{-1}
χ^2/dof	41.3/40

NOTE.—Errors are at 90% confidence level. All parameters of the model (including normalization) are best fitted with both *ASCA* and *Chandra* data points.

[a] Hydrogen column density.

[b] Temperature of electrons in a thin thermal plasma.

[c] Ionization parameter is an NEI.

[d] Metal abundances (helium fixed at cosmic). The elements included are C, N, O, Ne, Mg, Si, S, Ca, Fe, Ni.

[e] Observed flux in the 2.0–10.0 keV band.

[f] Absorption-corrected luminosity in the 2.0–10.0 keV band.

collectively, fixing the relative ratio to be solar (Anders & Grevesse 1989). Free parameters are the electron temperature (kT), the abundance (Z), the ionization parameter (nt), and interstellar absorption (N_H). For the other free parameter, we allow one normalization factor to be fitted to both the *ASCA* and *Chandra* fluxes simultaneously. The NEI fit is acceptable with the best-fit spectra and parameters shown in Figure 4 and Table 1. The data excess of *Chandra* and deficit of *ASCA* above and below the iron line are attributable to the gain uncertainty of these instruments. However, this small systematic difference is not a serious problem in the present analysis. The ionization parameter of $\tau = 1.7 \times 10^{10}$ cm^{-3} s is very small, while the abundance is significantly larger than the solar value.

4. DISCUSSION

ASCA discovered a diffuse X-ray source (G0.570−0.018) with a strong iron line near the Sgr B2 cloud; then *Chandra* found a ringlike structure of 10″ radius. The hydrogen column density is determined to be $N_H = 13.9^{+3.3}_{-3.2} \times 10^{22}$ H cm^{-2}. Since the N_H value is nearly equal to those of the Galactic center sources of the same Galactic latitude (Sakano 2000), G0.570−0.018 would be located near at the Galactic center region. We hence assume the source distance to be 8.5 kpc. The X-ray luminosity is then estimated to be $\simeq 10^{34}$ ergs, and the size of the ring radius is 0.4 pc. The spectra are well fitted with an NEI model with plasma temperature (kT) of 6.1 keV, ionization parameter (τ) of 1.7×10^{10} cm^{-3} s, and metal abundances (Z) of 4.5 $Z_\odot$. Therefore, together with the ringlike morphology, G0.570−0.018 is likely to be a young SNR, either in an adiabatic or a free expansion phase. We first apply a Sedov self-similar model, assuming it is in an adiabatic phase. This model gives the emission measure (EM $= n^2V$), radius (R), and electron temperature (kT) as follows (Ostriker et al. 1988):

$$n^2V = (4n_a)^2 4\pi R^2 \left(\frac{R}{12}\right) \quad (\mathrm{cm}^{-3}) ,$$

$$R = 5.0 \left(\frac{E}{10^{51}\ \mathrm{ergs}}\right)^{1/5} \left(\frac{n_a}{1\ \mathrm{cm}^{-3}}\right)^{-1/5} \left(\frac{t_s}{10^3\ \mathrm{yr}}\right)^{2/5} (\mathrm{pc}) ,$$

$$kT = 4.5 \left(\frac{E}{10^{51}\ \mathrm{ergs}}\right)^{2/5} \left(\frac{n_a}{1\ \mathrm{cm}^{-3}}\right)^{-2/5} \left(\frac{t_s}{10^3\ \mathrm{yr}}\right)^{-6/5} (\mathrm{keV}) ,$$

where t_s, n_a, and E are the age of the plasma (in unit of yr), ambient density (in units of cm^{-3}), and explosion energy of the supernova (in units of ergs), respectively. Using the observed values of $R = 0.4$ pc, $kT = 6.1$ keV, and EM $= 8.1 \times 10^{56}$ cm^{-3}, we obtain t_s, n_a, and E to be 70 yr, 5.1 cm^{-3}, and 3.5×10^{48} ergs, respectively. The swept-up mass is then calculated to be $M_H n_a (4/3)\pi R^3 \simeq 0.03\ M_\odot$, where M_H is mass of a hydrogen atom, which is much smaller than that of the SN ejecta of a few $M_\odot$. The estimated explosion energy of G0.570−0.018 is also extremely small compared with a usual SNR. These indicate that only a tiny fraction of the explosion energy ($\sim 10^{51}$ ergs) and ejected mass (a few $M_\odot$) have been converted to the thermal plasma. These facts strongly indicate that G0.570−0.018 is not in an adiabatic phase but still in a free expansion phase.

The X-ray ring structure of G0.570−0.018 is similar to that of SN 1987A (Burrows et al. 2000), where a strong stellar wind from a massive progenitor might produce a gas ring of subparsec radius, and was heated by the collision of supernova ejecta. From the radial profile in Figure 3, the thickness of the ring (FWHM) is about 6″, or 0.2 pc; hence, the plasma volume is 1.2×10^{55} cm^3. Since the X-ray flux from the ring is 67% of that of the whole area of G0.570−0.018, the emission measure from the ring is 5.5×10^{56} cm^{-3}. Then, using the best-fit ionization parameter (nt) of 1.7×10^{10} cm^{-3} s, the plasma density (n) and ionization age (t) of the X-ray ring are estimated to be 6.7 cm^{-3} and 80 yr, respectively. In Table 2 we compare the physical parameters of the ring of G0.570−0.018 with those of SN 1987A. The ring size and age are about 3–6 times larger than those of SN 1987A. Therefore, G0.570−0.018 would be a "future SN 1987A" after a free expansion with the expected speed of $v = R/t \simeq 4900$ km s^{-1}.

TABLE 2

COMPARISON OF THE PARAMETERS BETWEEN G0.570−0.018 AND SN 1987A

Source	Distance (kpc)	X-Ray Shell Radius (pc)	t (yr)
G0.570−0.018	8.5	0.4	80
SN 1987A	50[a]	0.12[a]	13

[a] The parameters of SN 1987A are taken from Burrows et al. 2000.

One problem of this scenario for G0.570−0.018 is an additional X-ray structure, the east-to-west X-ray tail. We suspect that the structure would be made by some instability of dense stellar wind from the progenitor, and was heated up by the collision of the SN ejecta. In this case, the front of the free-expanding ejecta would be about 2 times larger than the ring radius; hence, the age of SNR is doubled. This age is still in a very young phase; thus, the above discussion, which is based on a free expansion phase, is essentially not changed.

In the young SNR scenario, we expect nonthermal radio emissions associated with the thermal X-rays. However, we see no significant radio continuum flux from G0.570−0.018. In general, the X-ray flux is proportional to

the square of electron density (n^2), while the radio flux is proportional to the square of magnetic field B^2. Assuming that magnetic field is proportional to the ambient gas density (the magnetic field is frozen to the ambient gas), the flux ratio between X-ray to radio is roughly constant among shell-like SNRs. Referring the radio and X-ray data of typical young shell-like SNRs Cas A, Tycho and Kepler, we estimated the radio flux of G0.570−0.018 to be 0.1–1 Jy (except Cas A) at 1 GHz, using the X-ray flux of $\sim 10^{-12}$ ergs s^{-1}. SN 1987A has almost the same X-ray flux as that of G0.570−0.018, and the radio flux density is ∼40 mJy at 4.7 GHz (Burrows et al. 2000). This radio flux density would be below the current detection limit of the radio SNRs located near the GC, where the radio background is extremely high (∼0.1–0.5 Jy). Thus, we encourage more deep and fine spatial resolution searches for radio emissions near at G0.570−0.018.

We express our sincere thanks to T. Tsuru and M. Kohno for their contributions in the very early phase of this study and for stimulating discussions on this paper. The authors also thank Y. Maeda and M. Sakano for their useful discussions. H. Murakami is financially supported by the Japan Society for the Promotion of Science (JSPS).

REFERENCES

Anders, E., & Grevesse, N. 1989, Geochim. Cosmochim. Acta, 53, 197
Borkowski, K. J., Lyerly, W. J., & Reynolds, S. P. 2001, ApJ, 548, 820
Burke, B. E., Mountain, R. W., Harrison, D. C., Bautz, M. W., Doty, J. P., Ricker, G. R., & Daniels, P. J. 1991, IEEE Trans., ED-38, 1069
Burrows, D. N., et al. 2000, ApJ, 543, L149
Freeman, P. E., Kashyap, V., Rosner, R., & Lamb, D. Q. 2000, ApJ, submitted
Koyama, K., Awaki, H., Kunieda, H., Takano, S., & Tawara, Y. 1989, Nature, 339, 603
Koyama, K., Maeda, Y., Sonobe, T., Takeshima, T., Tanaka, Y., & Yamauchi, S. 1996, PASJ, 48, 249
Lis, D. C., & Carlstrom, J. E. 1994, ApJ, 424, 189
Mehlinger, M., Palmer, P., Goss, W. M., & Yuzef-Zadeh, F. 1993, ApJ, 412, 684
Mehlinger, M., Yuzef-Zadeh, F., Palmer, P., & Goss, W. M. 1992, ApJ, 401, 168
Murakami, H., Koyama, K., & Maeda, Y. 2001, ApJ, 558, 687
Murakami, H., Koyama, K., Sakano, M., Tsujimoto, M., & Maeda, Y. 2000, ApJ, 534, 283
Ohashi, T., et al. 1996, PASJ, 48, 157
Oka, T., Hasegawa, T., Hayashi, M., Handa, T., & Sakamoto, S. 1998a, ApJ, 493, 730
Oka, T., Hasegawa, T., Sato, F., Tsuboi, M., & Miyazaki, A. 1998b, ApJS, 118, 455
Ostriker, J. P., & McKee, C. F. 1988, Rev. Mod. Phys., 60, 1
Sakano, M. 2000, Ph.D. thesis, Kyoto Univ.
Sakano, M., et al. 1999, Proc. of the Japanese-German Workshop on High Energy Astrophysics, ed. W. Becker & M. Itoh (MPE Rep. 270; Garching bei München: MPE), 113
Seiradakis, J. H., Reich, W., Weilebinski, R., Lasenby, A. N., & Yusef-Zadeh, F. 1989, A&AS, 81, 291
Selemitsos, P. J., et al. 1995, PASJ, 47, 105
Tanaka, Y., Inoue, H., & Holt, S. S. 1994, PASJ, 46, L37
Townsley, L. K., Broos, P. S., Garmire, G. P., & Nousek, J. A. 2000, ApJ, 534, L139
Tsuboi, M., Handa, T., & Ukita, N. 1999, ApJS, 120, 1
Weisskopf, M. C., O'Dell, S. L., & Speybroeck, L. P. 1996, Proc. SPIE, 2805, 2
Yamauchi, S., Kawada, M., Koyama, K., Kunieda, H., Tawara, Y., & Hatsukade, I. 1990, ApJ, 365, 532